Available online at www.sciencedirect.com
ScienceDirect
Journal of Environmental Sciences 2010, 22(8) 1290–1296
JOURNAL OF ENVIRONMENTAL SCIENCES
ISSN 1001-0742
CN 11-2629/X
www.jesc.ac.cn

Activated carbon supported TiO_2-photocatalysis doped with Fe ions for continuous treatment of dye wastewater in a dynamic reactor

Youji Li*, Jun Chen, Jianben Liu, Mingyuan Ma, Wei Chen, Leiyong Li

College of Chemistry and Chemical Engineering, Jishou University, Jishou 416000, China. E-mail: bcclyj@163.com

Received 24 August 2009; revised 10 March 2010; accepted 18 March 2010

Abstract

Fe-doped TiO_2 coated on activated carbon (Fe-TiO_2/AC, FTA) composites were prepared by an improved sol-gel method and characterized by scanning electron microscopy, X-ray photoelectron spectroscopy, X-ray diffractometry, inductively coupled plasma mass spectrometry and BET surface area analysis. Obtained FTA composites were applied to the continuous treatment of dye wastewater in a dynamic reactor. The effects of Fe ion content, catalyst content, UV-lamp power and flowrate of the continuous treatment of dye wastewater on degradation efficiency were analyzed to determine the optimum operating conditions of dye wastewater degradation. Continuous photocatalytic experiments provided interesting results that FTA had a high chemical oxygen demand (COD) removal rate compared with TiO_2, Fe doped TiO_2 (FT) and TiO_2 coated on activated carbon (TA). In particular, when using the FTA catalyst with a Fe ion content of 0.33%, the kinetic content (k = 0.0376) of COD removal was more than the sum of both TA (0.0205) and 0.33% FT (0.0166). FTA showed a high photoactivity because of a synergistic effect between Fe ions and AC on TiO_2, which is higher than the individual effects of AC or Fe ions on TiO_2. Additionally, for the photocatalytic degradation of dye wastewater, the optimum Fe ion content, catalyst content, UV-lamp power and flowrate were 0.33%, 6 g/L, 60 W (two lamps) and 300 mL/hr, respectively. An investigation of catalyst reuse revealed that the 0.33% FTA showed almost no deactivation in photocatalytic degradation of naturally treated wastewater.

Key words: titanium dioxide; iron ions; activated carbon; dye wastewater; continuous treatment

DOI: 10.1016/S1001-0742(09)60252-7

Introduction

In recent years, there has been a great deal of interest in the use of advanced oxidation processes (AOPs) for the destruction of hazardous and refractory organic compounds because of the high oxidation potential of active oxygen species such as OH· and $O_2^{\bullet-}$, which are generated from irradiated semiconductor catalysts (Ollis et al., 1991; Huang et al., 1993; Mills and Hoffmann, 1993; Choi et al., 1994; Tennakone et al., 1997). The photocatalytic oxidation of toxic organic compounds through the use of TiO_2 semiconductors is an AOP emerging technology. TiO_2 is broadly used in environmental clean-up operations because of its non-toxic nature, photochemical stability and low cost, particularly when sunlight is used as the source of irradiation (Chen and Ray, 1998; Khodja et al., 2001). However, conventional TiO_2 powder has low conversion efficiency and is difficult to separate after photocatalysis (Holgado et al., 2000). To achieve rapid and efficient decomposition of organic pollutants and also easy manipulation of the catalyst in a total photocatalytic process, it may be effective to load TiO_2 nanoparticles onto suitably fine adsorbents and thus concentrate pollutants around the nanoparticles. Doping metal elements into TiO_2 may also strain the recombination of electron-hole pairs. Therefore, several photocatalytic studies have focused on the preparation of composites such as TiO_2/SiO_2, TiO_2/glass, TiO_2/zeolite and TiO_2-coated polystyrene spheres (Hilmi et al., 1999; Fabiyi and Skelton, 2000; Holgado et al., 2000; Phonthammachai et al., 2006). A different approach is to study the improvement of photoactivity using metal elements such Ag, Zn, Fe, Ce and Cu as dopants to modify TiO_2 (Grzechulska and Morawski, 2002; Tong et al., 2007; Sobana et al., 2008; Zhao et al., 2008; Zoltán et al., 2008). Most researchers have studied these approaches separately, whereas, it is significant to consider the synchronous influence of the support and the dopant on TiO_2 photoactivity.

In this work, we prepared Fe-TiO_2/activated carbon (FTA) composites by an improved sol-gel method. A continuous dye wastewater treatment in a dynamic reactor was adopted to evaluate the photoactivity of FTA composites. To further estimate FTA photoactivity, naturally treated wastewater was directly fed into the reactor to analyze their application lifetime. The aim of this study was to assess the photoactivity of FTA on the continuous treatment of dye wastewater.

* Corresponding author. E-mail: bcclyj@163.com

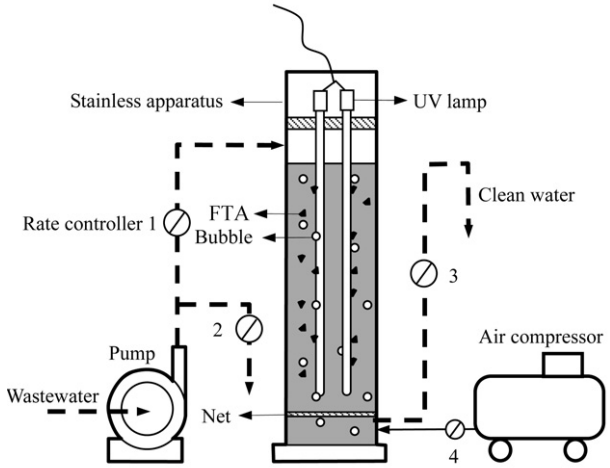

Fig. 1 Dynamic apparatus for the continuous photocatalytic treatment of wastewater.

1 Materials and methods

1.1 Materials

Tetrabutyl orthotitanate (analytical grade, Tixier Company, China), diethanolamine (analytical grade, Yifeng Company, China), iron nitrate (analytical grade, Xinli, China) and ethanol (analytical grade, Yangyuan Company, China) were used as received. Activated carbon grains (average particle size: 0.12 cm, surface area: 435.9 m^2/g, total pore volume: 0.08768 cm^3/g) were prepared by vapor activation of coconut shells.

1.2 Preparation of catalyst samples

The preparation of Fe doped TiO_2 coated on activated carbon (Fe-TiO_2/AC, FTA) composites was conducted as follows: a known amount of $Fe(NO_3)_3$ was dissolved in doubly-distilled water before the hydrolysis of $Ti(OC_4H_9)_4$. Tetrabutyl orthotitanate (8.5 mL) and diethanolamine (2.6 mL) were dissolved in ethanol. The solution was stirred at 20°C and then a mixture of $Fe(NO_3)_3$ solution desired amount of HCl, and ethanol was added. The resulting alkoxide solution was hydrolyzed and a Fe-TiO_2 sol was obtained. A desired amount of activated carbon was then added to the Fe-TiO_2 sol at a certain viscosity during ultrasonic treatment. When Fe-TiO_2 sol coated the support was changed into Fe-TiO_2 gel, the support was vacuum dried, and the obtained particles were heat-treated at 250°C for 2 hr in air and then at 500°C for 2 hr in nitrogen to prepare *n*% Fe-TiO_2/AC (*n*%FTA) composites, where *n*% indicates the mass ratio of Fe ions to TiO_2. In addition, TiO_2 powder, Fe-TiO_2 powder (FT), and TiO_2/AC (TA) composite were prepared as references using the same hydrolysis procedure.

1.3 Experimental operation system and analysis method

A flowchart of the continuous treatment process for the dye wastewater used in this study is illustrated in Fig. 1, which mainly consisted of a photocatalytic reactor, a net and two pumps.

A cylindrical photoreactor was produced using stainless steel with a height of 1000 mm and an inner diameter of 100 mm (dynamic photocatalytic reactor). This reactor had an effective volume of 6.3 L. The UV lamp was positioned at the center of the reactor and provided near UV radiation. Six air diffusers were mounted at the bottom of the reactor to ensure that excess O_2 was present and to maintain sufficient catalysts suspension in the reactor.

A perspex net acted as a filter and was placed about 50 mm above the bottom of the reactor. To keep catalysts within the reactor, millipore membrane filter paper of 85 mm diameter and pore sizes ranging in 0.2–0.4 μm were placed on the surface of the filter.

Two pumps were used to maintain the continuous treatment of the dye wastewater by the suspended catalysts. A recycling wastewater pump and an air compressor were used as part of the dynamic equipment.

The raw dye wastewater used in this study was collected from a dye factory in Hunan. Before the experiment, the wastewater was passed through a sand filter several times to remove suspended solids and the solution pH was adjusted to be within 7–8 by adding acid/base as required.

For the advanced photooxidation treatment process, wastewater was treated in a photoreactor contained suspended catalysts. The influent was continuously fed into the reactor from the top of reactor at a flowrate determined by two rate controllers 1 and 2 during the experiment. Effluent was removed from the bottom of the reactor at the same flow rate by controller 3. The aim was to keep wastewater molecules in the photoreactor for a certain time as determined by a theoretical calculation based on the reactor volume and the influent rate. During the continuous treatment process, the aeration rate was controlled by rate controller 4.

To investigate the effects of catalyst content and UV lamp electronic power on the photocatalytic degradation efficiency, a series of experiments were carried out under different photocatalytic conditions. Catalyst content was varied from 2 to 12 g/L. The UV lamp electronic power used was 25, 40, 60, 80 or 120 W. The aeration rate was controlled at 56 mL/sec for all experiments.

COD of the wastewater was measured according to standard methods (open reflux, dichromate titration method). The wastewater's color was measured with a colorimetry method.

1.4 Structural characterization

Obtained FTA composites were characterized by measuring their BET surface areas via the nitrogen absorption method (ASAP2010, Micromeritics, USA) at 77 K. The crystalline phase was identified by X-ray diffraction (Bruker, Germany) using Cu-$K\alpha$. radiation. Crystallite size was calculated from XRD measurements using Scherrer's equation. Morphologies were observed by SEM (JSM-5600LV, Japan). The chemical states of titanium, oxygen and iron in the composites were studied by X-ray photoelectron spectroscopy with a VG Scientific ESCALAB Mark spectrometer (England) and Mg$K\alpha$ radiation was used (1253.6 eV). X-ray photoelectron spectra were

Table 1 Description and characteristics of photocatalysts prepared by an improved sol-gel method

Sample[a]	Fe/TiO_2 (wt.%)	Surface area (m^2/g)	Total pore volume (cm^3/g)	Average diameter (nm)	Kinetic constant ($\times 10^3$ hr^{-1})
TiO_2	–	51.0	–	50	13.4
0.33% FT	0.33	67.2	–	30	16.6
TA	–	373.4	0.07487	25	20.5
0.33% FTA	0.33	348.6	0.07138	20	37.6
0.24% FTA	0.24	354.4	0.07143	23	23.9
0.56% FTA	0.56	338.7	0.07131	18	25.7

[a] Surface areas and total pore volumes of activated carbon are 435.9 m^2/g and 0.08768 cm^3/g, respectively. TiO_2 coating ratio of composites is about 10% with the relative error of ± 1%.
FT: Fe-TiO_2 power; TA: TiO_2/AC; FTA: Fe-TiO_2/AC.

referenced to the C1s peak (E_b = 285.0 eV). Fe content in TiO_2 was determined by high resolution inductively coupled plasma mass spectrometry (HR-ICP-MS, Micromass, England).

2 Results and discussion

2.1 Characteristics of the photocatalysts

The Fe content in TiO_2, surface areas and total pore volumes including that for the original activated carbon are summarized in Table 1, together with average diameters and kinetic constants. Surface areas of composites are evidently higher than that of pure TiO_2, indicating that the AC matrix had a relatively high surface area after loading with Fe-TiO_2 or TiO_2. As shown in Fig. 2a, the macropores and mesopores of AC are not blocked by Fe-TiO_2 nanoparticles. This is a possible reason why the 0.33% FTA composite has high surface area. To study the microstructure of Fe-TiO_2 nanoparticles on the AC surface, a selected region was magnified (Fig. 2b). White particles observed on composite surfaces are spherical TiO_2 particles doped with Fe ions, while multi-pore faces are amorphous AC. Compared to the agglomeration typical of pure TiO_2 (Fig. 2d), the spherical particles are well dispersed in the AC matrix because of the cumbering effect of AC on agglomeration of TiO_2 particles (Fig. 2b, c). In addition, we found that the 0.33% FTA composite had the smallest nanoparticle size compared to 0.33% FT powder and TiO_2 powder, this is attributed to the fact that Fe ions also act as barriers that control the growth of TiO_2 particles to a certain extent in addition to the AC matrix. XRD patterns of 0.33% FTA and pure TiO_2 are shown in Fig. 3. The XRD peak of the 101 crystal plane for anatase appears at 25.4° (2θ) and the 110 crystal plane for rutile appears at 27.5° (2θ) (Karunagaran et al., 2003).

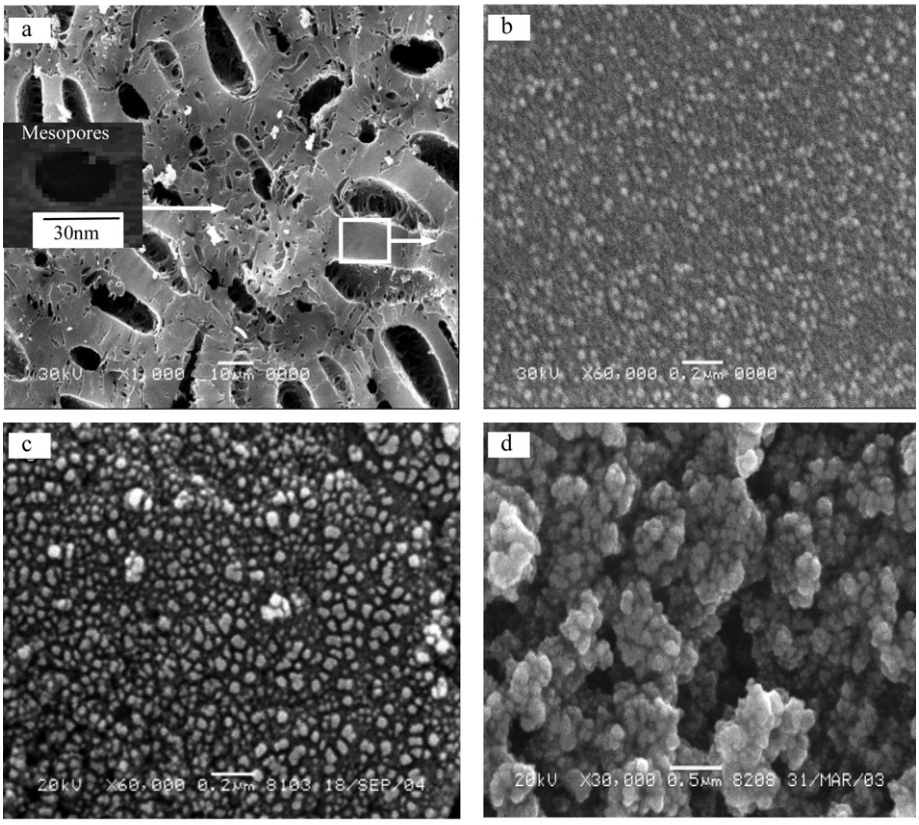

Fig. 2 SEM images of samples. (a) and (b) 0.33% FTA; (c) TA; (d) pure TiO_2.

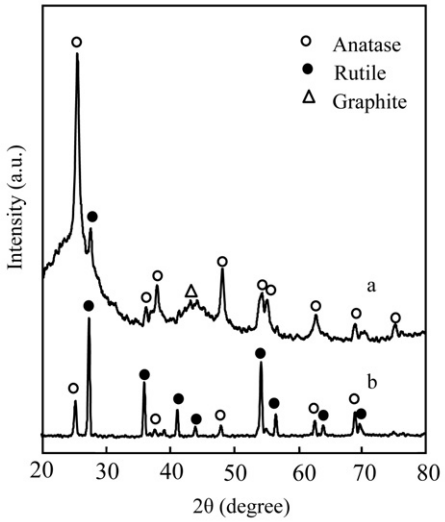

Fig. 3 XRD patterns of samples annealed at 500°C for 2 hr. Line a: 0.33% FTA; line b: pure TiO_2.

In addition, graphite was identified as the amorphous phases of activated carbon. No Fe peak was observed for the 0.33% FTA composite, probably due to the microscale nature of Fe ions and the similar radii of iron and titanium. It was indicated that Fe ions did not affect the crystalline structure of TiO_2 nanoparticles. Crystalline sizes of the Fe-TiO_2 in composites are about 20 nm, determined using Scherrer's equation and this is consistent with the SEM observation.

Figure 4 displays XPS spectra of 0.33% FTA. Irrespective of growth parameters, only lines characteristic of titanium, oxygen and carbon were observed with a small protuberance of iron. Binding energies of $Ti2p_{3/2}$ and $2p_{1/2}$ are the same as those of pure titanium at 459.4 and 465.3 eV, respectively. This shows the integrity of the TiO_2 structure and it was not modified by iron doping. Two XPS peaks correspond to two types of Fe species in the composites and this was obtained from XPS curve fitting of the Fe2p XPS peak, shown as an inset in Fig. 4. A binding energy of 709.2 eV is characteristic for FeO, while the higher binding energy of 710.6 eV is characteristic of Fe_2O_3. The coexistence of Fe^{3+} and Fe^{2+} can improve the photocatalytic efficiency according to the following Reactions (1) and (2):

$$Fe^{2+} + O_{ads} \longrightarrow Fe^{3+} + O^-_{ads} \quad (1)$$

$$Fe^{3+} + e^-_{cb} \longrightarrow Fe^{2+} \quad (2)$$

Fe^{3+} can trap photogenerated electrons in the conduction band and thus inhibit electron/hole pair recombination. On the other hand, Fe^{2+} can supply electrons to oxygen adsorbed on the surface of catalysts and accelerate the interfacial electron transfer (Molinari et al., 2000). However, the decreased activity observed above the optimum metal ions concentration is possibly due to oxidation of Fe^{2+} by hydroxyl radicals or holes:

$$Fe^{2+} + h^+ \longrightarrow Fe^{3+} \quad (3)$$

The correct doping content of Fe ions is thus essential for the improvement of TiO_2 photoactivity.

2.2 Photoactivity of catalysts

Experimental results for the decolorization and COD reduction of dye wastewater by photooxidation with different catalysts (dispersed with a content of 6 g/L) are illustrated in Fig. 5. We found that the disappearance of color occurred more readily than COD reduction for all catalysts. Dye chemicals are usually composed of molecules with large molecular structures. When the chromophore on the dye structure is degraded the color will disappear but COD reduction is not significant until the main structure of molecule is oxidized to final products such as CO_2. Under identical experimental conditions, we found that the wastewater photodegradation rate for the different catalysts decreased as follows: 0.33% FTA > TA > 0.33% FT > TiO_2. This sequence suggests that a synergistic effect between the activated carbon and Fe ions is important. The high surface area of activated carbon, which works well as an effective adsorbent, concentrates dye molecules around the loaded TiO_2. Fe ions, used as dopants, play a role in improving the photoinduced charge separation in the nanostructured semiconductor and in the interfacial charge transfer process at the semiconductor/solution interface.

2.3 Effect of catalyst content

The effect of the amount of FTA in the photocatalytic solution on the COD reduction of dye wastewater is shown

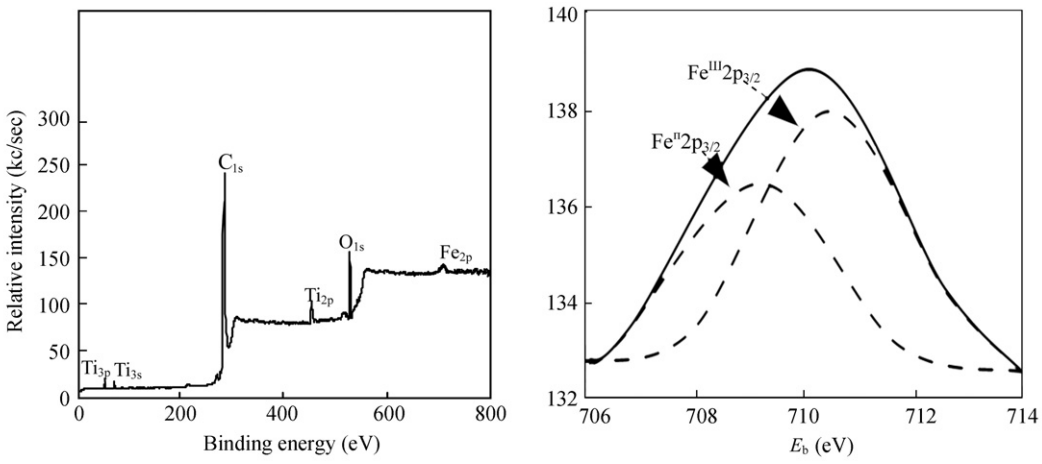

Fig. 4 XPS spectra of 0.33% FTA. Right figure: high resolution XPS spectrum of the Fe2p region.

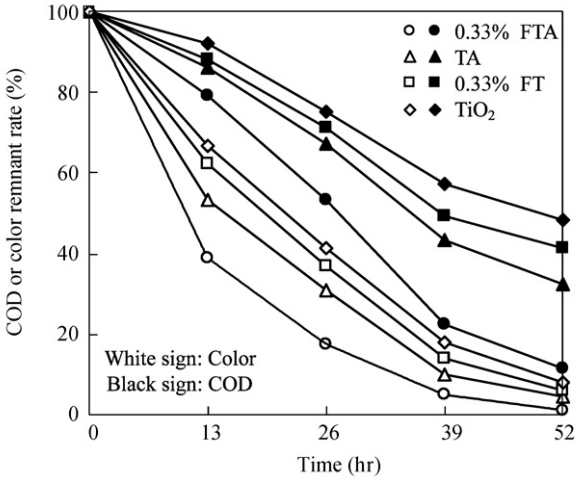

Fig. 5 Dye wastewater COD removal by different catalysts. I_0 = 60 W (two lamps), Q = 56 mL/sec, flowrate = 150 mL/hr, catalysts content = 6 g/L.

in Fig. 6. The COD removal rate of dye wastewater solutions increases with an increasing catalyst content until a plateau is reached at concentrations of 6.0 g/L and subsequently decreases. It seems that there is a limit above which no improvement is obtained by increasing the amount of catalyst. A similar observation was made by other researchers (Li and Zhao, 1999; Sobana et al., 2008) when studying Reactive Flumequine and Reactive Red 23. The turbidity of the solution above 6.0 g/L reduced the light transmission through the solution, while below this level the adsorption on TiO_2 surface and the absorption of light by TiO_2 were the limiting factors. It was reported that the catalyst concentration has both positive and negative impact on the photodecomposition rate (Neppolian et al., 2002; Harrelkas et al., 2008). The increased concentration of catalyst increases the quantity of photons absorbed and consequently the degradation rate. Further increase in catalyst concentration beyond 6.0 g/L may result in the deactivation of activated molecules due to collision with the ground state molecules and increased turbidity of the solution reduced the light transmission through.

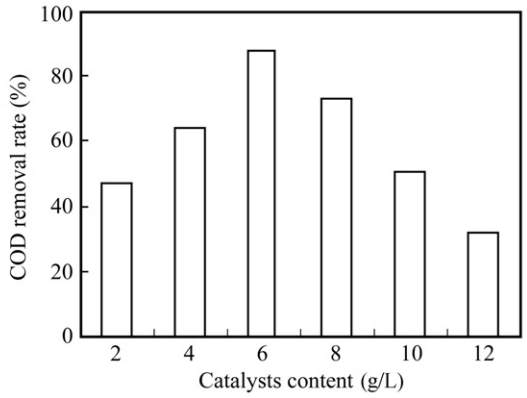

Fig. 6 Dye wastewater COD removal by 0.33% FTA. I_0 = 60 W (two lamps), Q = 56 mL/sec, flowrate = 150 mL/hr.

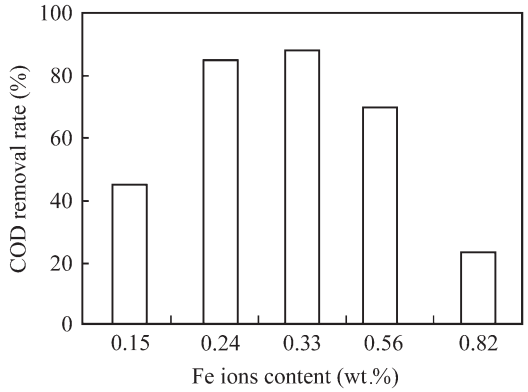

Fig. 7 Dye wastewater COD removal by FTA with different Fe ion contents. I_0 = 60 W (two lamps), Q = 56 mL/sec, flowrate =150 mL/hr, catalyst content = 6 g/L.

2.4 Effect of iron ions concentration

Photocatalytic decomposition results of samples with different iron content are shown in Fig. 7. We observed that the decomposition of wastewater must be related to catalyst structure. The relationship between the DOC removal rate and the catalysts with different Fe ions doping content follows the sequence: 0.33% FTA > 0.24% FTA > 0.56% FTA > 0.15% FTA > 0.82% FTA. These results show a significant effect of Fe ions content on the photocatalytic degradation of dye wastewater. Fe ions can have a positive influence on TiO_2 photocatalysis when Fe ions content is less than 0.33%, whereas it can have a negative influence on TiO_2 photocatalysis when the Fe ions content is more than 0.33%. This is mainly due to the effect of Fe ions content on the electron/hole pair separation and hydroxyl radicals or holes producing.

2.5 Effect of UV lamp electric power

Light intensity is a major factor in photocatalytic reactions because electron-hole pairs are produced by light energy (Tsoukleris et al., 2007). A direct relationship exists between the electric power of a UV lamp and its light intensity if the UV lamp in the reactor is stationary (Fig. 1b). The electric power of the UV lamp thus influences the degradation of dye wastewater. To investigate the effect of UV-lamp power on the DOC removal rate of dye wastewater, two sets of experiments were conducted using either one or two UV lamps. Results are shown in Fig. 8. We observed that the degradation of dye wastewater rapidly increases with an increase in UV lamp electronic power until a plateau is reached at 60 W and then a slow increase is observed. Identical relationships exist between the COD removal rate and the electronic power when using one UV lamp or two UV lamps. Additionally, when the UV lamp was used at a low electronic power such as 25, 40 and 60 W, the two UV lamp experiment had twice the removal rate of COD compared to the experiment with one UV lamp. From an economical point of view, a UV lamp power of 60 W was selected for the dye wastewater degradation experiments.

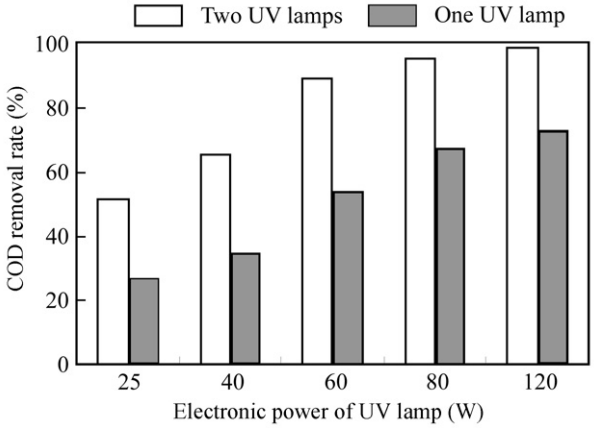

Fig. 8 Dye wastewater COD removal by 0.33% FTA with different UV lamp electronic power. Q = 56 mL/sec, flowrate = 150 mL/hr, catalyst content = 6 g/L.

2.6 Effect of flowrate in photocatalytic process

As shown in Fig. 9, the flowrate has an important effect on the COD removal rate of dye wastewater. The COD removal rate of dye wastewater decreases when the flowrate increases under continuous operating conditions.

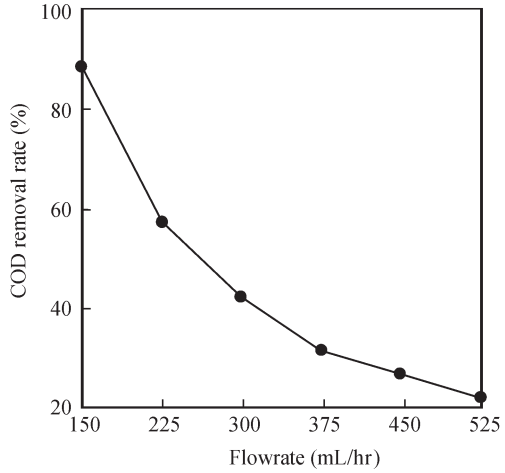

Fig. 9 Dye wastewater COD removal by 0.33% FTA with different flowrates. I_0 = 60 W (two lamps), Q = 56 mL/sec, catalyst content = 6 g/L.

This is mainly attributed to the decrease of photocatalytic time. With flowrates of 150, 225, 300, 375, 450 and 525 mL/hr dye wastewater, molecules were exposed to ultraviolet radiation for 42, 28, 21, 17, 14 and 12 hr by theoretical calculations, respectively. The degradation efficiency of dye wastewater should be considered on the basis of compliance with wastewater draining standards. To reduce cost of electric power and meet the dye wastewater draining standards, the optimum flowrate is 300 mL/hr for adequate and cost-effective degradation of dye wastewater.

2.7 Kinetics reaction

In the photocatalytic oxidation process, the COD removal rate is proportional to the content of the organic compound (pollutant) and this is indirectly expressed by chemical oxygen demand. Therefore, based on the experimental data, a kinetic equation for COD removal was obtained to describe the dye wastewater photocatalytic degradation.

$$r = -\frac{\mathrm{d[COD]}}{\mathrm{d}t} = k[\mathrm{COD}] \tag{4}$$

$$\ln\frac{[\mathrm{COD}]_0}{[\mathrm{COD}]_t} = \ln\frac{C_0}{C_t} = k \cdot t \tag{5}$$

where, C_0 (mg/L) is the initial COD of the effluents and C_t is the COD value at time t. The slope of the $\ln\frac{C_t}{C_0}$ versus time plot gives the value for the rate constant k in hr^{-1} as listed in Table 1. The rate constant (k) of FTA is higher than that of TiO_2, TA or FT. Furthermore, with optimum Fe ions doping content the rate constant (k = 0.0376) of 0.33% FTA is more than the sum of both TA (0.0205) and 0.33% FT (0.0166). This result indicates that coexistence of the AC and Fe ions has a synergistic effect on improving the photoactivity of TiO_2, which is more than the individual effect of AC or Fe ions.

2.8 Photocatalytic degradation of naturally treated wastewater

To further verify the activity and lifetime of FTA, the reaction equipment was connected to a drainpipe from a municipal sewage plant in Hunan. Results are presented in Fig. 10a. COD values of naturally treated wastewater

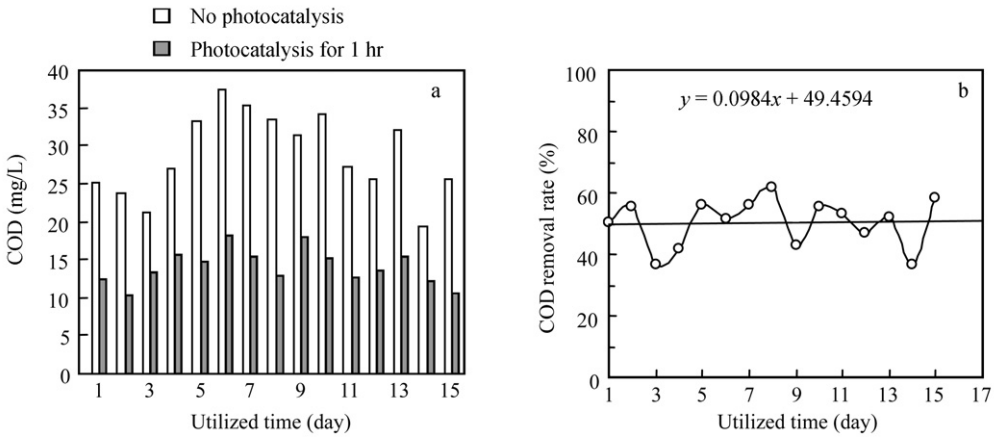

Fig. 10 COD comparison for photocatalysis (a) and changes of COD removal ratio (b) in the pilot continuous experiment using 0.33% FTA. I_0 = 60 W (two lamps), Q = 56 mL/sec, catalyst content = 6 g/L.

are found to be variable because municipal sewage contains different organic pollutants with time. For 0.33% FTA catalysts, the COD of naturally treated wastewater decreased with different utilization time. This suggests that the lifetime of the activated carbon carriers in FTA increased greatly and that used catalysts retained high photocatalytic activity. This was mainly because the activated carbon was not blocked for the Fe-TiO_2 decomposition of organic pollutants while the activated carbons provided a high concentration of organic compounds for the Fe-TiO_2 distributed on them by the absorption process. A progressive equation $y = 0.0984x + 49.4594$ was found by linear analysis to describe the relationship between COD removal rate and the utilization time of the catalysts (Fig. 10b). This equation indicates that the utilization time of the catalysts hardly affects the COD removal rate.

3 Conclusions

Because of a synergistic effect between Fe ions and activated carbon on TiO_2 photocatalysts, the degradation efficiency of dye wastewater by four photocatalysts changes as follows: 0.33% FTA > TA > 0.33% FT > TiO_2. The rate constant ($k = 0.0376$) of 0.33% FTA is found to be more than the sum of the rate constants of both TA (0.0205) and 0.33% FT (0.0166). Among the catalysts, 0.33% FTA composites have the highest photoactivity because of its high surface area, multiphase purity and low electron/hole pairs recombination rate as well as having the optimum content of doped Fe ions. The photocatalytic degradation of dye wastewater depends on the catalyst content, doped Fe ions content, UV lamp electronic power and flowrate. For the photocatalytic degradation of dye wastewater, the optimum Fe ions content, catalyst content, UV-lamp power and flowrate affecting the DOC removal rate were 0.33%, 6 g/L, 60 W (two lamps) and 300 mL/hr, respectively. Furthermore, the same FTA catalyst can be used for a number of cycles which will reduce the operating cost of the continuous treatment of natural treated wastewater.

Acknowledgments

This work was supported by the National Natural Science Foundation of China (No. 50802034), the Educational and Technological Department of Hunan Province (No. 08B063) and the Natural Science Foundation of Hunan Province (No. 09JJ6101).

References

Chen D, Ray A K, 1998. Photodegradation kinetics of 4-nitrophenol in TiO_2 suspensions. *Water Research*, 32: 3223–3234.

Choi W, Termin A, Hoffmann M R, 1994. The role of metal ion dopants in quantum-sized TiO_2: correlation between photoreactivity and charge carrier recombination dynamics. *Journal of Physical and Chemistry*, 98: 13669–13679.

Fabiyi M E, Skelton R L, 2000. Photocatalytic mineralisation of Methylene Blue using buoyant TiO_2-coated polystyrene beads. *Journal of Photochemical and Photobiology A: Chemistry*, 132(1-2): 121–128.

Grzechulska J, Morawski A W, 2002. Photocatalytic decomposition of azo-dye Acid Black 1 in water over modified titanium dioxide. *Applied Catalysis B: Environment*, 36: 45–51.

Harrelkas F, Paulo A, Alves M M, El Khadir L, Zahraa O, Pons M N, 2008. Photocatalytic and combined anaerobic-photocatalytic treatment of textile dyes. *Chemosphere*, 72(11): 816–1822.

Hilmi A, Luong J H T, Nguyen A L, 1999. Utilization of TiO_2 deposited on glass plates for removal of metals from aqueous wastes. *Chemosphere*, 38(4): 865–874.

Holgado M, Cintas A, Ibisate M, Serna C J, Lopez C, Meseguer F, 2000. Three-dimensional arrays formed by monodisperse TiO_2 coated on SiO_2 spheres. *Journal of Colloid Interface Science*, 229: 6–11.

Huang C P, Dong C, Tang Z, 1993. Advanced chemical oxidation: Its present role and potential future in hazardous waste treatment. *Waste Management*, 13: 361–377.

Karunagaran B, Kumar R T, Kumar V S, Mangalaraj D, Narayandass Sa K, Rao G M, 2003. Structural characterization of DC magnetron-sputtered TiO_2 thin films using XRD and Raman scattering studies. *Materials Science in Semiconductor Processing*, 6(5-6): 547–550.

Khodja A A, Sehili T, Pilichowski J F, Boule P, 2001. Photocatalytic degradation of 2-phenylphenol on TiO_2 and ZnO in aqueous suspensions. *Journal of Photochemical and Photobiology A: Chemistry*, 141: 231–239.

Li X Z, Zhao Y G, 1999. Advanced treatment of dyeing wastewater for reuse. *Water Science Technology*, 39: 249–255.

Mills G, Hoffmann M R, 1993. Photocatalytic degradation of pentachlorophenol on titanium dioxide particles: identification of intermediates and mechanism of reaction. *Environmental Science and Technology*, 27: 1681–1689.

Molinari A, Amadelli R, Antolini L, Maldotti A, Battioni P, Mansuy D, 2000. Phororedox and photocatalytic processes on Fe(III)-porphyrin surface modified nanocrystalline TiO_2. *Journal of Molecular Catalysis A: Chemical*, 158(2): 521–531.

Neppoliana B, Choi H C, Sakthivel S, Banumathi A, Murugesan V, 2002. Solar/UV-induced photocatalytic degradation of three commercial textile dyes. *Journal of Hazardous Materials*, 89: 303–317.

Ollis D F, Pelizzetti E, Serpone N, 1991. Photocatalyzed destruction of water contaminants. *Environmental Science and Technology*, 25: 1522–1529.

Phonthammachai N, Krissanasaeranee M, Gulari E, Jamieson A M, Wongkasemjit S, 2006. Crystallization and catalytic activity of high titanium loaded TS-1 zeolite. *Materials Chemistry and Physics*, 97(2-3): 458–467.

Sobana N, Selvam K, Swaminathan M, 2008. Optimization of photocatalytic degradation conditions of Direct Red 23 using nano-Ag doped TiO_2. *Separation and Purification Technology*, 62(3): 648–653.

Tennakone K, Tilakaratne C T K, Kottegoda I R M, 1997. Photomineralization of carbofuran by TiO_2-supported catalyst. *Water Research*, 31: 1909–1912.

Tong T Z, Zhang J L, Tian B Z, Chen F, He D N, Anpo M, 2007. Preparation of Ce-TiO_2 catalysts by controlled hydrolysis of titanium alkoxide based on esterification reaction and study on its photocatalytic activity. *Journal of Colloid and Interface Science*, 315(1): 382–388.

Tsoukleris D S, Maggos T, Vassilakos C, Falaras P, 2007. Photocatalytic degradation of volatile organics on TiO_2 embedded glass spherules. *Catalysis Today*, 129(1-2): 96–101.

Zhao Y, Li C Z, Liu X H, Gu F, Du H L, Shi L Y, 2008. Zn-doped TiO_2 nanoparticles with high photocatalytic activity synthesized by hydrogen-oxygen diffusion flame. *Applied Catalysis B: Environmental*, 79(3): 208–215.

Zoltán A, Nándor B, Tnde A, Gyula W, Pál S, András D et al., 2008. Synthesis, structure and photocatalytic properties of Fe(III)-doped TiO_2 prepared from $TiCl_3$. *Applied Catalysis B: Environmental*, 81(1-2): 27–37.